

Goals of the Homework

- Solve partial differential equations.
- Experiment stability of explicit time integration schemes.
- Parallelize the code using MPI (and optionally combine MPI with OpenMP).

Intermediate deadline: 26/11/2021. FDTD code without parallelization.

Statement

The propagation of electromagnetic waves is governed by Maxwell's equations, which describe the behavior of electromagnetic fields. Without sources, Maxwell's equations read as follows:

$$\frac{\partial \mathbf{B}}{\partial t} + \mathbf{curl} \mathbf{E} = 0, \quad (1)$$

$$\frac{\partial \mathbf{D}}{\partial t} - \mathbf{curl} \mathbf{H} = 0, \quad (2)$$

where, in three dimensions and assuming a Cartesian coordinate system and MKS units, $\mathbf{B} = \mathbf{B}(x, y, z, t)$ is the magnetic flux density (in T), $\mathbf{E} = \mathbf{E}(x, y, z, t)$ is the electric field (in V/m), $\mathbf{D} = \mathbf{D}(x, y, z, t)$ is the electric displacement field (in C/m²) and $\mathbf{H} = \mathbf{H}(x, y, z, t)$ is the magnetic field (in A/m). These four vector fields are function of the position (x, y, z) and of time t . In linear materials the following constitutive laws link these fields:

$$\mathbf{B} = \mu \mathbf{H}, \quad (3)$$

$$\mathbf{D} = \epsilon \mathbf{E}, \quad (4)$$

where the constants μ and ϵ denote the magnetic permeability and the dielectric permittivity, respectively. The speed of light in the material is $c = \frac{1}{\sqrt{\epsilon\mu}}$. In vacuum, $\mu = \mu_0 = 4\pi \cdot 10^{-7}$ H/m and $\epsilon_0 \approx 8.854 \cdot 10^{-12}$ F/m. The speed of light in vacuum is $c_0 = \frac{1}{\sqrt{\epsilon_0\mu_0}} \approx 3 \cdot 10^8$ m/s.

You are asked to solve Maxwell's equations in a three-dimensional domain of size $a \times b \times d$. Your work will consist in a validation phase and in a simulation phase. In the validation phase you will solve a resonant cavity problem and compare the numerical solution with its analytical solution. A resonant cavity is essentially an empty metallic box. In the simulation phase you will simulate a microwave oven, energized through a waveguide port on a side of the cavity.

The electromagnetic energy enters the domain via a rectangular aperture on one of the sides of the oven, which models the end of a waveguide bringing the electromagnetic energy from the magnetron to the inside of the microwave oven cavity. The electromagnetic field enters the oven as a TE_{10} mode.

The numerical scheme to solve the problem is the Finite Difference Time Domain technique, first proposed by Kane S. Yee in 1966 (see the Appendix).

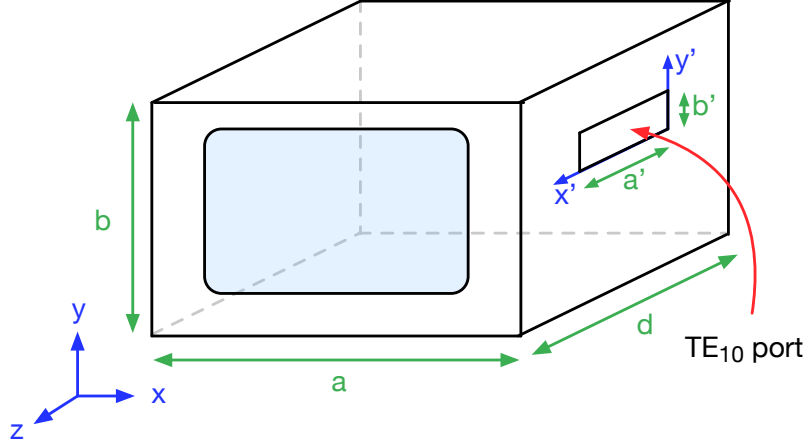


Figure 1: A microwave oven can be modelled as a metallic box with a rectangular aperture from which the electromagnetic energy enters. The aperture is the end of a waveguide in which the electromagnetic field travels in the TE_{10} mode.

The FDTD scheme relies on the discretization of the electric and magnetic fields in space and time, on dual grids. The discrete unknowns are (refer to the Figure 1 of the paper in the Appendix):

- the x -component of \mathbf{E} (denoted by E_x) on grid points $(i + 1/2, j, k)$, $i = \{0, N_x - 1\}$, $j = \{0, N_y\}$, $k = \{0, N_z\}$, at time steps n , with $n = \{1, 2, \dots\}$. Notice that the E_x unknowns are located in the midpoint of the edges along x ;
- the y -component of \mathbf{E} (denoted by E_y) on grid points $(i, j + 1/2, k)$, $i = \{0, N_x\}$, $j = \{0, N_y - 1\}$, $k = \{0, N_z\}$, at time steps n , with $n = \{1, 2, \dots\}$. Notice that the E_y unknowns are located in the midpoint of the edges along y ;
- the z -component of \mathbf{E} (denoted by E_z) on grid points $(i, j, k + 1/2)$, $i = \{0, N_x\}$, $j = \{0, N_y\}$, $k = \{0, N_z - 1\}$, at time steps n , with $n = \{1, 2, \dots\}$. Notice that the E_z unknowns are located in the midpoint of the edges along z ;
- the x -component of \mathbf{H} (denoted by H_x) on grid points $(i, j + 1/2, k + 1/2)$, $i = \{0, N_x\}$, $j = \{0, N_y - 1\}$, $k = \{0, N_z - 1\}$ at time steps $n + 1/2$, $n = \{1, 2, \dots\}$. Notice that the H_x unknowns are located on the faces parallel to the yz plane;
- the y -component of \mathbf{H} (denoted by H_y) on grid points $(i + 1/2, j, k + 1/2)$, $i = \{0, N_x - 1\}$, $j = \{0, N_y\}$, $k = \{0, N_z - 1\}$ at time steps $n + 1/2$, $n = \{1, 2, \dots\}$. Notice that the H_y unknowns are located on the faces parallel to the xz plane;
- the z -component of \mathbf{H} (denoted by H_z) on grid points $(i + 1/2, j + 1/2, k)$, $i = \{0, N_x - 1\}$, $j = \{0, N_y - 1\}$, $k = \{0, N_z\}$ at time steps $n + 1/2$, $n = \{1, 2, \dots\}$. Notice that the H_z unknowns are located on the faces parallel to the xy plane.

Remembering that the curl operator can be expanded as

$$\mathbf{curl} \mathbf{A} = \begin{vmatrix} \hat{i} & \hat{j} & \hat{k} \\ \frac{\partial}{\partial x} & \frac{\partial}{\partial y} & \frac{\partial}{\partial z} \\ A_x & A_y & A_z \end{vmatrix} = \hat{i} \left(\frac{\partial A_z}{\partial y} - \frac{\partial A_y}{\partial z} \right) + \hat{j} \left(\frac{\partial A_x}{\partial z} - \frac{\partial A_z}{\partial x} \right) + \hat{k} \left(\frac{\partial A_y}{\partial x} - \frac{\partial A_x}{\partial y} \right), \quad (5)$$

we use finite differences to approximate the spatial and temporal derivatives and obtain a discrete scheme. For example, the update equation for E_x is

$$\begin{aligned} E_x^{n+1}(i+1/2, j, k) &= E_x^n(i+1/2, j, k) \\ &+ \frac{\Delta t}{\epsilon \Delta y} \left(H_z^{n+1/2}(i+1/2, j+1/2, k) - H_z^{n+1/2}(i+1/2, j-1/2, k) \right) \\ &- \frac{\Delta t}{\epsilon \Delta z} \left(H_y^{n+1/2}(i+1/2, j, k+1/2) - H_y^{n+1/2}(i+1/2, j, k-1/2) \right), \end{aligned} \quad (6)$$

and the update equation for H_x is

$$\begin{aligned} H_x^{n+1/2}(i, j+1/2, k+1/2) &= H_x^{n-1/2}(i, j+1/2, k+1/2) \\ &+ \frac{\Delta t}{\mu \Delta z} \left(E_y^n(i, j+1/2, k+1) - E_y^n(i, j+1/2, k) \right) \\ &- \frac{\Delta t}{\mu \Delta y} \left(E_z^n(i, j+1, k+1/2) - E_z^n(i, j, k+1/2) \right). \end{aligned} \quad (7)$$

For this homework it will be assumed that the grid step is equal in all directions, i.e. $\Delta x = \Delta y = \Delta z$. For the validation phase, you will consider homogeneous Dirichlet boundary conditions on the whole boundary. For the simulation phase, you will need to impose a specific electric field on a portion of the boundary.

Instructions

By group of **two students** (this is mandatory) you are asked to:

1. Write the remaining FDTD update equations for E_y , E_z , H_y and H_z .
2. Write a C program that solves the discretized equations in parallel with MPI. Optionally you can also combine MPI with OpenMP. You are completely free to imagine how to split the computation for the parallel implementations. Several approaches are possible: prefer simple solutions and document your choices.
3. A cavity can resonate at discrete modes indexed by the integers m , n and l (note that here n is a mode index and is not related to the n appearing in the update equations), and the generic TE resonant mode is usually denoted as TE_{mnl} . Validate your code by simulating the TE_{101} resonant mode of a cavity with dimensions $a \times b \times d$:

(a) Impose the initial condition

$$E_y = \sin\left(\frac{m\pi x}{a}\right) \sin\left(\frac{l\pi z}{d}\right),$$

and run your simulation (note that all the other field components are zero). Verify that you obtain a field corresponding to the analytical solution

$$\begin{cases} E_y = \cos(2\pi f_{mnl}t) \sin\left(\frac{m\pi x}{a}\right) \sin\left(\frac{l\pi z}{d}\right) \\ H_x = Z_{TE}^{-1} \sin(2\pi f_{mnl}t) \sin\left(\frac{m\pi x}{a}\right) \cos\left(\frac{l\pi z}{d}\right) \\ H_z = -\frac{\pi}{\omega\mu a} \sin(2\pi f_{mnl}t) \cos\left(\frac{m\pi x}{a}\right) \sin\left(\frac{l\pi z}{d}\right) \end{cases} \quad (8)$$

where ω is the angular frequency. The resonant frequency of the TE_{mnl} mode is computed as

$$f_{mnl} = \frac{c}{2\pi} \sqrt{\left(\frac{m\pi}{a}\right)^2 + \left(\frac{n\pi}{b}\right)^2 + \left(\frac{l\pi}{d}\right)^2},$$

whereas the impedance is computed as

$$Z_{TE} = \frac{\omega\mu}{\sqrt{\omega^2\mu\epsilon - \left(\frac{m\pi}{a}\right)^2 - \left(\frac{n\pi}{b}\right)^2}},$$

where ω is the angular frequency. Be sure to report the computed values of f_{mnl} and Z_{TE} in your report, as well as the dimensions a , b and d you chose for your cavity.

- (b) Compute the total electromagnetic energy inside the cavity at every timestep and verify that it is conserved along the simulation. Verify that the total energy is $W = \epsilon abd/8$. What can you say about the ratio between the energy in H_x and the energy in H_z when $a = b = d$? Provide a plot of energy vs. time. Remember that electric and magnetic energies in the domain Ω are computed as

$$W_e = \frac{1}{2} \int_{\Omega} \epsilon |\mathbf{E}|^2 dV, \quad W_m = \frac{1}{2} \int_{\Omega} \mu |\mathbf{H}|^2 dV.$$

4. Test the stability of the FDTD scheme in by varying the spatial step and the time step. Compare your findings with the theoretical stability criterion from the Appendix (equations (7) and (8)).
5. Implement the source as a waveguide port. Electromagnetic fields propagate in waveguides in discrete modes indexed by the numbers m and n . In TE modes, the electric field is tangent to the transverse section of the waveguide, and we will consider a TE_{10} mode. The source will be a region of size $a' = 0.1m \times b' = 0.05m$ on one of the sides of your domain. If you chose to place the port as depicted in Figure 1, your source field will have only the $E_{y'}$ and $H_{x'}$ components ($E_{x'} = H_{y'} = 0$) with the expression

$$E_{y'} = \sin(2\pi ft) \sin\left(\frac{x'\pi}{a'}\right), \quad H_{x'} = -Z_{TE}^{-1} \sin(2\pi ft) \sin\left(\frac{x'\pi}{a'}\right), \quad f = 2.45 \text{ GHz}.$$

Note that the axis y' is redundant and equal to y , it is there just to remark that the source is applied on a 2D surface.

6. Perform a scalability analysis of your parallel code, by evaluating both the strong and weak scaling.
7. Do a rough analysis of the arithmetic intensity of the FDTD and discuss which is the main limiting factor for the speed of your algorithm. What do you expect if you run the FDTD on a machine capable of 250 GB/s of memory bandwidth and 1.3 TFLOPS/s of processing power?

Input file format Your program must take as argument on the command line a parameter file (*e.g.* `param.dat`), written in ASCII, with the following structure:

a
b
d
Δx
Δt
T_f
S
v

where a, b and d are the side-lengths of the computational domain, Δx ($= \Delta y = \Delta z$) is the spatial step, Δt is the time step, T_f is the final simulation time, and S is the sampling rate at which the results should be saved to disk ($S = 1$ corresponds to saving all the time steps). The parameter v takes the values 0 and 1, 0 corresponds to validation mode and 1 to computation mode.

Output file format The output files should be created using the Silo library. See https://gitlab.onelab.info/mcicuttin/snippets/-/blob/master/silo_example/silo.c
In order to use the library on NIC5, load the appropriate modules with

```
module load releases/2020b Silo/4.11-foss-2020b
```

Send your report (max. 10 pages of text; additional figures can be appended) by email to anthony.royer@uliege.be, matteo.cicuttin@uliege.be and cgeuzaine@uliege.be in PDF format together with your C code and SLURM submission script. The files (report, C code, SLURM script) should be named

```
project2_Lastname.pdf
project2_Lastname.c
project2_Lastname.sh
```

You should provide code that compiles and runs on NIC5 when the environment from `releases/2020b` is loaded. When you send us your code, give us the exact command line to compile it on NIC5 and, if necessary, the list of additional modules you loaded.

General remarks on C coding style

Your coding style *will* be evaluated. As such, some quality in the submitted code is expected, and you should strive to have a clean and neat coding style. In general, think about who will read your code and ask yourself if it is clear and understandable. If you do that, you will be fine. You must also beware of some mistakes that, if done, *will* cost you points.

- Do all your computations in double. There is no reason to use single precision in this project.
- If you `malloc()` something, remember to `free()` it.
- Check return values for failure, especially from `malloc()`, `open()` or similar calls. Don't assume that those calls will always succeed.
- Don't use Variable Length Arrays, i.e.

```
int function(int N) {  
    int array[N];  
}
```

Really, don't. The value of `N` must be known at compile time. If it is not the case, use `malloc()`.

- Don't abuse comments. If something is obvious, don't comment it. If you feel the need to comment some code, ask yourself if perhaps you can write the code in a clearer way instead of putting that comment.
- Use `assert()`. Check array access with it. Check loop invariants with it. Once you think you have sufficient `assert()`s in your code, put some more. And remember that `assert()` is a debug facility that goes away in release builds, so don't use it to validate user input.
- Try to use relevant and appropriate variable and function names. Be coherent in naming stuff, in order to make it easy to track down where data goes.
- A function *should* fit in your screen. If it doesn't, perhaps you should break it. If you have a function that takes more than 5 parameters, perhaps you need to think if you really need all of them. If a function takes more than 10 parameters, there's most likely a problem.
- Do not use global variables. There are very few valid use cases for global variables and they are one of the factors that make your code not thread safe.

Appendix

V. CONCLUSION

The characteristics of the waves guided along a plane interface which separates a semi-infinite region of free space from that of a magnetoionic medium are investigated for the case in which the static magnetic field is oriented perpendicular to the plane interface. It is found that surface waves exist only when $\omega_c < \omega_p$ and that also only for angular frequencies which lie between ω_c and $1/\sqrt{2}$ times the upper hybrid resonant frequency. The surface waves propagate with a phase velocity which is always less than the velocity of electromagnetic waves in free space. The attenuation rates normal to the interface of the surface wave fields in both the media are examined. Numerical results of the surface wave characteristics are given for one typical case.

REFERENCES

- [1] P. S. Epstein, "On the possibility of electromagnetic surface waves," *Proc. Nat'l Acad. Sciences*, vol. 40, pp. 1158-1165, December 1954.
- [2] T. Tamir and A. A. Oliner, "The spectrum of electromagnetic waves guided by a plasma layer," *Proc. IEEE*, vol. 51, pp. 317-332, February 1963.
- [3] M. A. Gintsburg, "Surface waves on the boundary of a plasma in a magnetic field," *Rasprost. Radiovoln i Ionosf., Trudy NIZMIRAN USSR*, no. 17(27), pp. 208-215, 1960.
- [4] S. R. Seshadri and A. Hessel, "Radiation from a source near a plane interface between an isotropic and a gyrotropic dielectric," *Canad. J. Phys.*, vol. 42, pp. 2153-2172, November 1964.
- [5] G. H. Owyang and S. R. Seshadri, "Guided waves propagating along the magnetostatic field at a plane boundary of a semi-infinite magnetoionic medium," *IEEE Trans. on Microwave Theory and Techniques*, vol. MTT-14, pp. 136-144, March 1966.
- [6] S. R. Seshadri and T. T. Wu, "Radiation condition for a magnetoionic medium," to be published.

Numerical Solution of Initial Boundary Value Problems Involving Maxwell's Equations in Isotropic Media

KANE S. YEE

Abstract—Maxwell's equations are replaced by a set of finite difference equations. It is shown that if one chooses the field points appropriately, the set of finite difference equations is applicable for a boundary condition involving perfectly conducting surfaces. An example is given of the scattering of an electromagnetic pulse by a perfectly conducting cylinder.

INTRODUCTION

SOLUTIONS to the time-dependent Maxwell's equations in general form are unknown except for a few special cases. The difficulty is due mainly to the imposition of the boundary conditions. We shall show in this paper how to obtain the solution numerically when the boundary condition is that appropriate for a perfect conductor. In theory, this numerical attack can be employed for the most general case. However, because of the limited memory capacity of present day computers, numerical solutions to a scattering problem for which the ratio of the characteristic linear dimension of the obstacle to the wavelength is large still seem to be impractical. We shall show by an example that in the case of two dimensions, numerical solutions are practical even when the characteristic length of the

obstacle is moderately large compared to that of an incoming wave.

A set of finite difference equations for the system of partial differential equations will be introduced in the early part of this paper. We shall then show that with an appropriate choice of the points at which the various field components are to be evaluated, the set of finite difference equations can be solved and the solution will satisfy the boundary condition. The latter part of this paper will specialize in two-dimensional problems, and an example illustrating scattering of an incoming pulse by a perfectly conducting square will be presented.

MAXWELL'S EQUATION AND THE EQUIVALENT SET OF FINITE DIFFERENCE EQUATIONS

Maxwell's equations in an isotropic medium [1] are:¹

$$\frac{\partial \mathbf{B}}{\partial t} + \nabla \times \mathbf{E} = 0, \quad (1a)$$

$$\frac{\partial \mathbf{D}}{\partial t} - \nabla \times \mathbf{H} = \mathbf{J}, \quad (1b)$$

$$\mathbf{B} = \mu \mathbf{H}, \quad (1c)$$

$$\mathbf{D} = \epsilon \mathbf{E}, \quad (1d)$$

Manuscript received August 24, 1965; revised January 28, 1966. This work was performed under the auspices of the U. S. Atomic Energy Commission.

The author is with the Lawrence Radiation Lab., University of California, Livermore, Calif.

¹ In MKS system of units.

where J , μ , and ϵ are assumed to be given functions of space and time.

In a rectangular coordinate system, (1a) and (1b) are equivalent to the following system of scalar equations:

$$-\frac{\partial B_x}{\partial t} = \frac{\partial E_z}{\partial y} - \frac{\partial E_y}{\partial z}, \quad (2a)$$

$$-\frac{\partial B_y}{\partial t} = \frac{\partial E_x}{\partial z} - \frac{\partial E_z}{\partial x}, \quad (2b)$$

$$\frac{\partial B_z}{\partial t} = \frac{\partial E_x}{\partial y} - \frac{\partial E_y}{\partial x}, \quad (2c)$$

$$\frac{\partial D_x}{\partial t} = \frac{\partial H_z}{\partial y} - \frac{\partial H_y}{\partial z} - J_x, \quad (2d)$$

$$\frac{\partial D_y}{\partial t} = \frac{\partial H_x}{\partial z} - \frac{\partial H_z}{\partial x} - J_y, \quad (2e)$$

$$\frac{\partial D_z}{\partial t} = \frac{\partial H_y}{\partial x} - \frac{\partial H_x}{\partial y} - J_z, \quad (2f)$$

where we have taken $\mathbf{A} = (A_x, A_y, A_z)$. We denote a grid point of the space as

$$(i, j, k) = (i\Delta x, j\Delta y, k\Delta z) \quad (3)$$

and for any function of space and time we put

$$F(i\Delta x, j\Delta y, k\Delta z, n\Delta t) = F^n(i, j, k). \quad (4)$$

A set of finite difference equations for (2a)–(2f) that will be found convenient for perfectly conducting boundary condition is as follows.

For (2a) we have

$$\frac{B_x^{n+1/2}(i, j + \frac{1}{2}, k + \frac{1}{2}) - B_x^{n-1/2}(i, j + \frac{1}{2}, k + \frac{1}{2})}{\Delta t} = \frac{E_y^n(i, j + \frac{1}{2}, k + 1) - E_y^n(i, j + \frac{1}{2}, k)}{\Delta z} - \frac{E_z^n(i, j + 1, k + \frac{1}{2}) - E_z^n(i, j, k + \frac{1}{2})}{\Delta y}. \quad (5)$$

The finite difference equations corresponding to (2b) and (2c), respectively, can be similarly constructed.

For (2d) we have

$$\frac{D_x^n(i + \frac{1}{2}, j, k) - D_x^{n-1}(i + \frac{1}{2}, j, k)}{\Delta t} = \frac{H_z^{n-1/2}(i + \frac{1}{2}, j + \frac{1}{2}, k) - H_z^{n-1/2}(i + \frac{1}{2}, j - \frac{1}{2}, k)}{\Delta y} - \frac{H_y^{n-1/2}(i + \frac{1}{2}, j, k + \frac{1}{2}) - H_y^{n-1/2}(i + \frac{1}{2}, j, k - \frac{1}{2})}{\Delta z} + J_x^{n-1/2}(i + \frac{1}{2}, j, k). \quad (6)$$

The equations corresponding to (2e) and (2f), respectively, can be similarly constructed.

The grid points for the E -field and the H -field are chosen so as to approximate the condition to be discussed below as accurately as possible. The various grid positions are shown in Fig. 1.

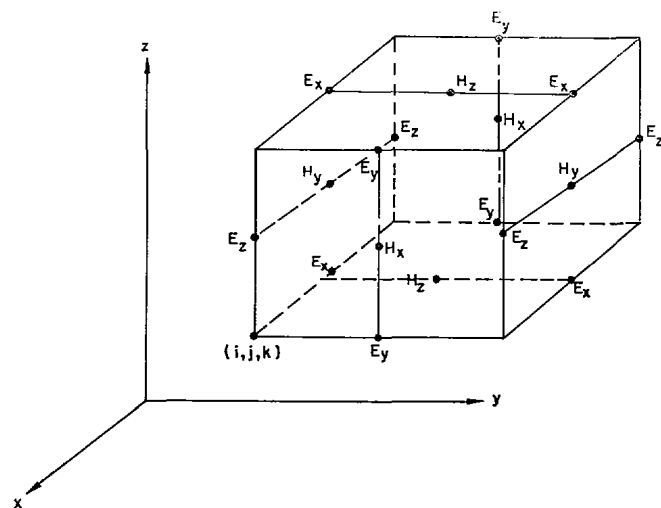


Fig. 1. Positions of various field components. The E -components are in the middle of the edges and the H -components are in the center of the faces.

BOUNDARY CONDITIONS

The boundary condition appropriate for a perfectly conducting surface is that the tangential components of the electric field vanish. This condition also implies that the normal component of the magnetic field vanishes on the surface. The conducting surface will therefore be approximated by a collection of surfaces of cubes, the sides of which are parallel to the coordinate axes. Plane surfaces perpendicular to the x -axis will be chosen so as to contain points where E_y and E_z are defined. Similarly, plane surfaces perpendicular to the other axes are chosen.

GRID SIZE AND STABILITY CRITERION

The space grid size must be such that over one increment the electromagnetic field does not change significantly. This means that, to have meaningful results, the linear dimension of the grid must be only a fraction of the wavelength. We shall choose $\Delta x = \Delta y = \Delta z$. For computational stability, it is necessary to satisfy a relation between the space increment and time increment Δt . When ϵ and μ are variables, a rigorous stability criterion is difficult to obtain. For constant ϵ and μ , computational stability requires that

$$\sqrt{(\Delta x)^2 + (\Delta y)^2 + (\Delta z)^2} > c\Delta t = \sqrt{\frac{1}{\epsilon\mu}} \Delta t, \quad (7)$$

where c is the velocity of light. If c_{\max} is the maximum light velocity in the region concerned, we must choose

$$\sqrt{(\Delta x)^2 + (\Delta y)^2 + (\Delta z)^2} > c_{\max}\Delta t. \quad (8)$$

This requirement puts a restriction on Δt for the chosen Δx , Δy , and Δz .

MAXWELL'S EQUATIONS IN TWO DIMENSIONS

To illustrate the method, we consider a scattering problem in two dimensions. We shall assume that the field components do not depend on the z coordinate of a

point. Furthermore, we take ϵ and μ to be constants and $J \equiv 0$. The only source of our problem is then an "incident" wave. This incident wave will be "scattered" after it encounters the obstacle. The obstacle will be of a few "wavelengths" in its linear dimension. Further simplification can be obtained if we observe the fact that in cylindrical coordinates we can decompose any electromagnetic field into "transverse electric" and "transverse magnetic" fields if ϵ and μ are constants. The two modes of electromagnetic waves are characterized by

1) Transverse electric wave (TE)

$$\begin{aligned} H_x = H_y = 0, \quad E_z = 0, \\ -\mu \frac{\partial H_z}{\partial t} = \frac{\partial E_y}{\partial x} - \frac{\partial E_x}{\partial y}, \\ \epsilon \frac{\partial H_z}{\partial y} = \frac{\partial E_x}{\partial t}, \quad -\frac{\partial H_z}{\partial x} = \epsilon \frac{\partial E_y}{\partial t}, \end{aligned} \quad (9)$$

and

2) Transverse magnetic wave (TM)

$$\begin{aligned} E_x = E_y = 0, \quad H_z = 0, \\ \epsilon \frac{\partial E_z}{\partial t} = \frac{\partial H_y}{\partial x} - \frac{\partial H_x}{\partial y}, \\ \mu \frac{\partial H_x}{\partial t} = -\frac{\partial E_z}{\partial y}, \quad \mu \frac{\partial H_y}{\partial t} = \frac{\partial E_z}{\partial x}. \end{aligned} \quad (10)$$

Let C be a perfectly conducting boundary curve. We approximate it by a polygon whose sides are parallel to the coordinate axes. If the grid dimensions are small compared to the wavelength, we expect the approximation to yield meaningful results.

Letting

$$\tau = ct = \sqrt{\frac{1}{\mu\epsilon}} t \quad (11)$$

and

$$Z = \sqrt{\frac{\mu}{\epsilon}} = 376.7, \quad (12)$$

we can write the finite difference equations for the TE and TM waves.

TE waves:

$$\begin{aligned} H_z^{n+1/2}(i + \frac{1}{2}, j + \frac{1}{2}) = H_z^{n-1/2}(i + \frac{1}{2}, j + \frac{1}{2}) \\ - \frac{1}{Z} \frac{\Delta\tau}{\Delta x} [E_y^n(i + 1, j + \frac{1}{2}) - E_y^n(i, j + \frac{1}{2})] \\ + \frac{1}{Z} \frac{\Delta\tau}{\Delta y} [E_x^n(i + \frac{1}{2}, j + 1) - E_x^n(i + \frac{1}{2}, j)] \end{aligned} \quad (13a)$$

$$E_x^{n+1}(i + \frac{1}{2}, j) = E_x^n(i + \frac{1}{2}, j)$$

$$+ Z \frac{\Delta\tau}{\Delta y} [H_z^{n+1/2}(i + \frac{1}{2}, j + \frac{1}{2}) - H_z^{n+1/2}(i + \frac{1}{2}, j - \frac{1}{2})] \quad (13b)$$

$$\begin{aligned} E_y^{n+1}(i, j + \frac{1}{2}) = -Z \frac{\Delta\tau}{\Delta x} [H_z^{n+1/2}(i + \frac{1}{2}, j + \frac{1}{2}) \\ - H_z^{n+1/2}(i - \frac{1}{2}, j + \frac{1}{2})]. \end{aligned} \quad (13c)$$

TM waves:

$$\begin{aligned} E_z^{n+1}(i, j) = E_z^n(i, j) \\ + Z \frac{\Delta\tau}{\Delta x} [H_y^{n+1/2}(i + \frac{1}{2}, j) - H_y^{n+1/2}(i - \frac{1}{2}, j)] \\ - Z \frac{\Delta\tau}{\Delta y} [H_x^{n+1/2}(i, j + \frac{1}{2}) - H_x^{n+1/2}(i, j - \frac{1}{2})] \end{aligned} \quad (14a)$$

$$\begin{aligned} H_x^{n+1/2}(i, j + \frac{1}{2}) = H_x^{n-1/2}(i, j + \frac{1}{2}) \\ - \frac{1}{Z} \frac{\Delta\tau}{\Delta y} [E_z^n(i, j + 1) - E_z^n(i, j)] \end{aligned} \quad (14b)$$

$$\begin{aligned} H_y^{n+1/2}(i + \frac{1}{2}, j) = H_y^{n-1/2}(i + \frac{1}{2}, j) \\ + \frac{1}{Z} \frac{\Delta\tau}{\Delta x} [E_z^n(i + 1, j) - E_z^n(i, j)]. \end{aligned} \quad (14c)$$

NUMERICAL COMPUTATIONS FOR TM WAVES

For further numerical discussion we shall limit ourselves to the TM waves. In this case we use the finite difference equations (14a)–(14c). The values for $E_z^0(i, j)$, $H_y^{1/2}(i + \frac{1}{2}, j)$, and $H_x^{1/2}(i, j - \frac{1}{2})$ are obtained from the incident wave.² Subsequent values are evaluated from the finite difference equations (14a)–(14c). The boundary condition is approximated by putting the boundary value of $E_z^n(i, j)$ equal to zero for any n .

To be specific, we shall consider the diffraction of an incident TM wave by a perfectly conducting square. The dimensions of the obstacle, as well as the profile of the incident wave, are shown in Fig. 2.

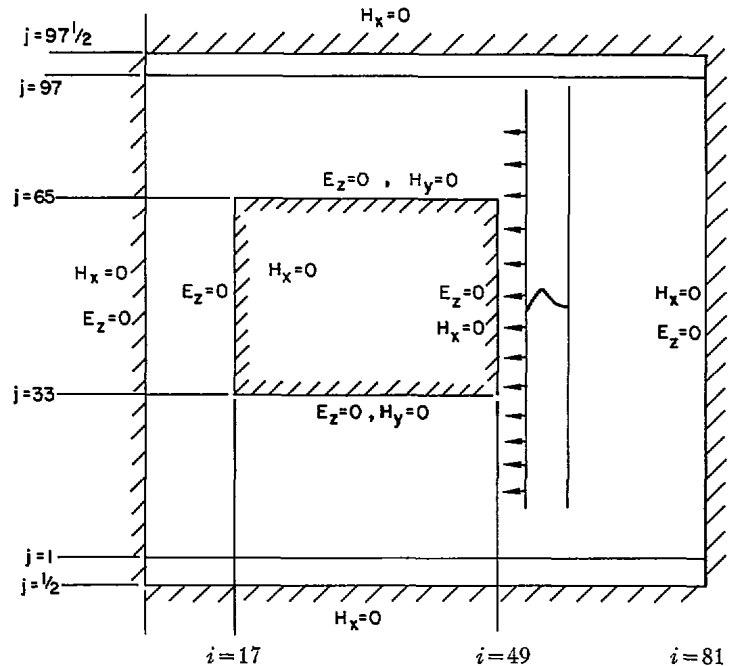


Fig. 2. Equivalent problem for scattering of a TM wave.

² We choose t such that when $t=0$ the incident wave has not encountered the obstacle.

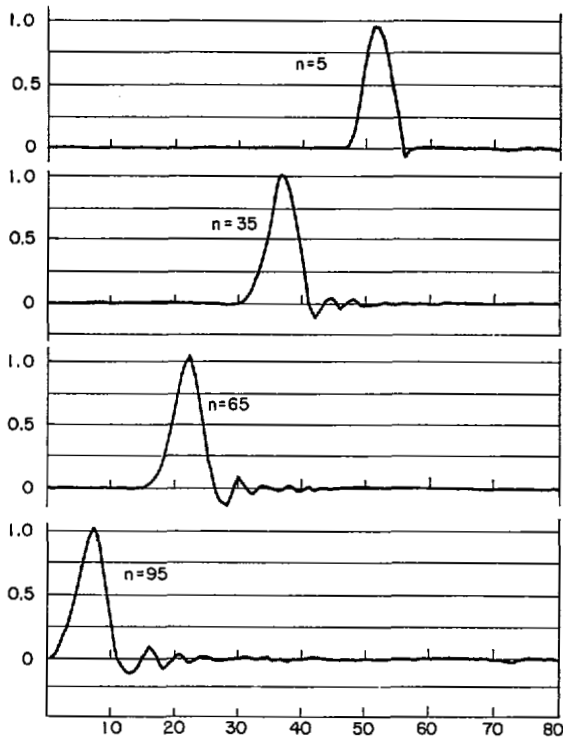


Fig. 3. Results of the calculation of E_z by means of (14a)-(14c) in the absence of the obstacle. The ordinate is in volts/meter and the abscissa is the number of horizontal increments. n is the number of time cycles.

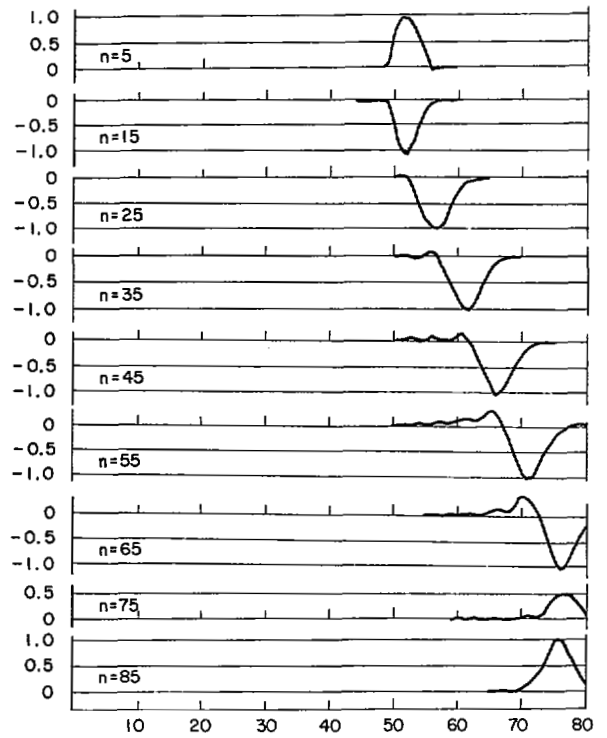


Fig. 5. E_z of the TM wave for various time cycles. $j=50$.

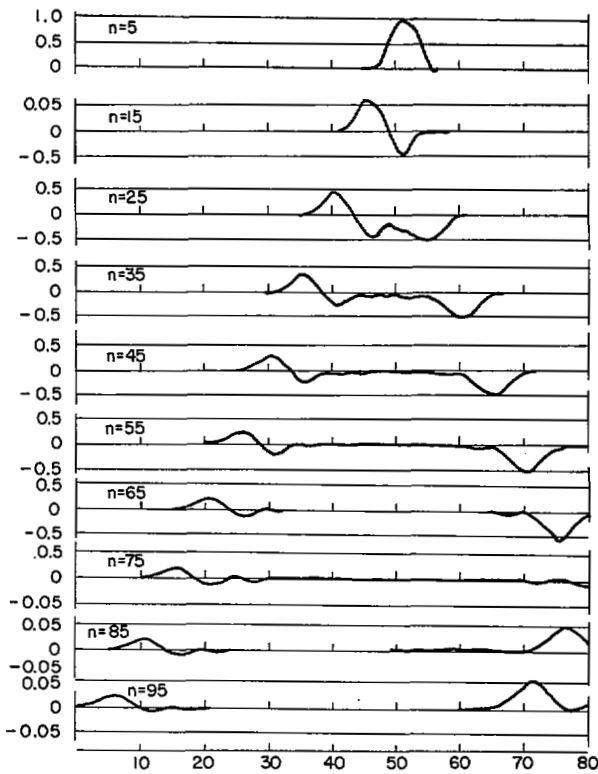


Fig. 4. E_z of the TM wave in the presence of the obstacle for various time cycles when $j=30$.

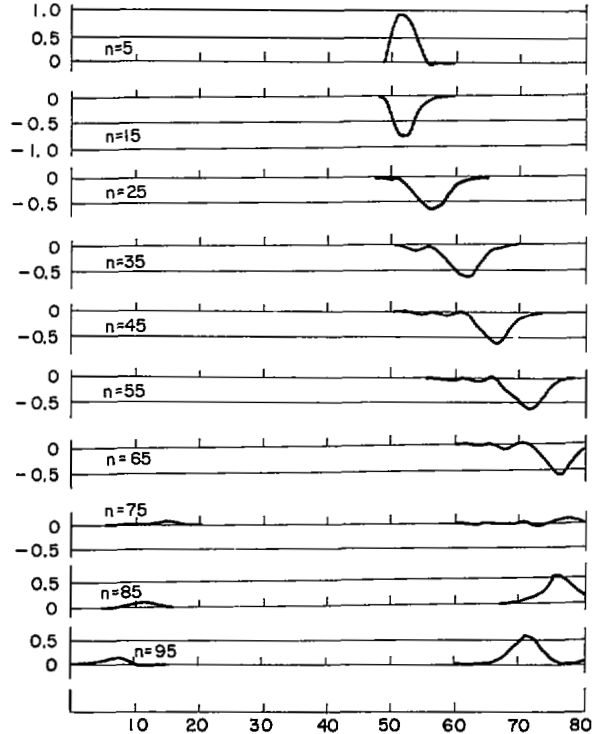


Fig. 6. E_z of the TM wave for various time cycles. $j=65$.

Let the incident wave be plane, with its profile being a half sine wave. The width of the incident wave is taken to be α units and the square has sides of length 4α units. Since the equations are linear, we can take $E_z = 1$ unit. The incident wave will have only an E_z component and an H_y component. We choose

$$\Delta x = \Delta y = \alpha/8 \quad (15a)$$

and

$$\Delta \tau = c\Delta t = \frac{1}{2}\Delta x = \alpha/16. \quad (15b)$$

A finite difference scheme over the whole x - y plane is impractical; we therefore have to limit the extent of our calculation region. We assume that at time $t=0$, the left traveling plane wave is "near" the obstacle. For a *restricted* period of time, we can therefore replace the original problems by the equivalent problem shown in Fig. 2.

The input data are taken from the incident wave with

$$E_z(x, y, t) = \sin \left[\frac{(x - 50\alpha + ct)\pi}{8\alpha} \right] \\ 0 \leq x - 50\alpha + ct \leq 8\alpha \quad (16a)$$

$$H_y(x, y, t) = \frac{1}{Z} E_z(x, y, t). \quad (16b)$$

From the differential equation satisfied by E_z we conclude that the results for the equivalent problem (see Fig. 2) should approximate those of the original problems, provided

$$0 \leq n\Delta\tau \leq 64\Delta\tau,$$

because the artificial boundary conditions will not affect our solution for this period of time.

For $n > 64$, however, only on certain points will the results of the equivalent problems approximate those of the original problems.

Numerical results are presented for the TM waves discussed above. To gain some idea of the accuracy of the finite difference equation, we have used the system (14a)–(14c) with the initial E_z being a half sine wave for the case of no obstacle. We note that the outer boundary conditions will not affect this incident wave as there is no H_x component in the incident wave. Ninety-five time cycles were run with the finite difference system (14a)–(14c), and the machine output is shown in Fig. 3. The oscillation and the widening of the initial pulse is due to the imperfection of the finite difference system.

Figure 4 shows the value of E_z of the TM wave as a function of the horizontal grid coordinate i for a fixed vertical grid coordinate $j=30$. At the end of five time cycles, the wave just hits the obstacle. The line $j=30$ does not meet the obstacle, but is "sufficiently" near the obstacle to be affected by a "partially reflected" wave. There is also a partially transmitted wave. The phase of the reflected wave is opposite that of the incident wave, as required by the boundary condition of the obstacle. There should also be a decrease in wave amplitude due to cylindrical divergence, but the cal-

culatation was not carried far enough to show this effect.

Figure 5 shows the value of E_z for the TM wave as a function of the horizontal grid coordinate i for $j=50$. This line ($j=50$) meets the obstacle, and hence we expect a reflected wave going to the right. These expectations are borne out in Fig. 5. After the reflected wave from the object meets the right boundary (see Fig. 2), the wave is reflected again. This effect is shown for the time cycles 75, 85, and 95.

Figure 6 is for $j=65$. This line forms part of the boundary of the obstacle. Because of the required boundary condition, E_z is zero on the boundary point. To the right of the obstacle there is a "partially" reflected wave of about half the amplitude of a fully reflected wave. To the left of the obstacle there is a "transmitted" wave after 85 time cycles.

All these graphs were obtained by means of linear interpolation between the grid points. They have been redrawn for reproduction.

COMPARISON OF THE COMPUTED RESULTS WITH THE KNOWN RESULTS ON DIFFRACTION OF PULSES BY A WEDGE

There exist no exact results for the particular example we considered here. However, in the case when the obstacle is a wedge, Keller and Blank [2] and Friedlander [3] have solved the diffraction problem in closed forms. In addition, Keller [4] has also proposed a method to treat diffraction by polygonal cylinders. To carry out the method proposed by Keller [4], one would have to use some sort of finite difference scheme. The present difference scheme seems to be simpler to apply in practice. For a restricted period of time and on a restricted region, our results should be identical with those obtained from diffraction by a wedge. We present such a comparison along the points on the straight line coincident with the upper edge (i.e., $j=65$).

Let the sides of a wedge coincide with the rays $\theta=0$ and $\theta=\beta$. Let the physical space be $0 < r < \infty$, $0 < \theta < \beta$. Let this wedge be perfectly conducting. If the incident E_z is given by

$$E_z^{\text{inc}} = f \left\{ t + \frac{r}{c} \cos(\theta - \theta_0) \right\},$$

where θ_0 is the direction of incidence, Friedlander [3] has shown that the solution to this diffraction problem is

$$E_z(r, \theta, t) = \sigma(\theta - \theta_0) f \left\{ t + \frac{r}{c} \cos(\theta - \theta_0) \right\} \\ - \sigma(\theta + \theta_0) f \left\{ t + \frac{r}{c} \cos(\theta + \theta_0)^* \right\} \\ - \frac{1}{2\beta} \int_0^\infty \left\{ Q(\theta - \theta_0, \xi) - Q(\theta + \theta_0, \xi) \right\} \\ \cdot f \left(t - \frac{r}{c} \cosh \xi \right) d\xi, \quad (17)$$

11

* $(\theta + \theta_0)^* = (\theta + \theta_0) + 2m\beta$; where m is an integer so chosen that $-\beta < (\theta + \theta_0)^* \leq \beta$.

where

$$\begin{aligned} \sigma(\psi) &= 1 \quad (|\psi| < \pi); \\ \sigma(\psi) &= 0 \quad (\pi < |\psi| < \beta); \\ \sigma(\psi + 2\beta) &= \sigma(\psi) \end{aligned}$$

and

$$k = \frac{\pi}{\beta}$$

$$Q(\psi, \xi) = - \frac{\sin k(\pi + \psi)}{\cosh k\xi - \cos k(\pi + \psi)} - \frac{\sin k(\pi - 4)}{\cosh k\xi - \cos k(\pi - 4)}.$$

At $t=0$, the incident wave hits the corner.

The discontinuities of the first two terms across the lines $\theta = \theta_0 \pm \pi$ and $\theta = -\theta_0 \pm \pi$ are compensated for by the contributions from the last integral. It can be shown that for

$$\theta = \theta_0 = \frac{\pi}{2}; \quad \beta = \frac{3\pi}{2}$$

$$E_z\left(r, \frac{\pi}{2}, t\right) = f\left(t + \frac{r}{2}\right) - \frac{1}{2}f\left(t - \frac{r}{c}\right) - \frac{\sqrt{3}}{2\pi} \int_0^\infty \frac{f\left(t - \frac{r}{c} \cosh \xi\right)}{\cosh k\xi + \frac{1}{2}} d\xi. \quad (18)$$

For our incident wave we have⁴

⁴ The origin of the wedge is taken to be the upper right-hand corner of the square. The zero time here differs from that of the numerical integration.

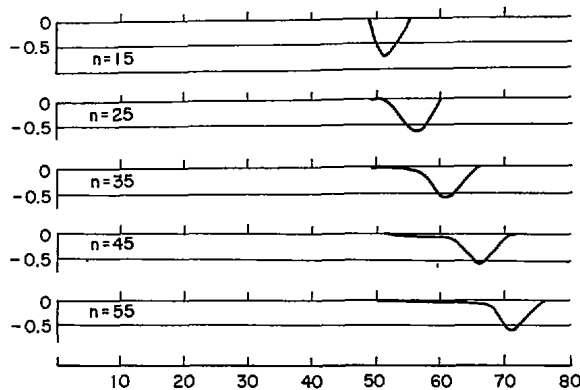


Fig. 7. Calculation of E_z for various cycles. These results are based on (18). The origin of the coordinate and of the time have been adjusted to agree with that used in the numerical calculation.

$$f(t) = \begin{cases} 0 < \frac{c\pi t}{\alpha} < 8 \\ 0 & \text{otherwise.} \end{cases}$$

Results of the computations based on (18) are shown in Fig. 7. The agreement with the graphs on Fig. 6 appears to be good, even for this coarse grid spacing.

ACKNOWLEDGMENT

The author wishes to thank Dr. C. E. Leith for helpful discussions and to express his gratitude to H. Barnett and W. P. Crowley for their assistance in the course of making the numerical calculations.

REFERENCES

- [1] J. Stratton, *Electromagnetic Theory*. New York: McGraw-Hill, 1941, p. 23.
- [2] J. B. Keller and A. Blank, "Diffraction and reflection of pulses by wedges and corners," *Commun. Pure Appl. Math.*, vol. 4, pp. 75-94, June 1951.
- [3] F. G. Friedlander, *Sound Pulses*. New York: Cambridge, 1958.
- [4] J. B. Keller, *Electromagnetic Waves*. Madison, Wis.: Univ. of Wisconsin Press, 1961.